TERRESTRIAL VOLCANIC AND IMPACT ANALOGS TO SMALL MARTIAN CRATERS: UTILIZING REMOTE SENSING AND FIELD-BASED DATASETS TO ANALYZE FORMATIONAL AND SEDIMENT TRANSPORT PROCESSES. V. M. Peet[1], M. S. Ramsey[1], and D. A. Crown[2], [1]Department of Geology and Planetary Science, University of Pittsburgh, Pittsburgh, PA 15260, vmp10@pitt.edu, ramsey@ivis.eps.pitt.edu, [2]Planetary Science Institute, 1700 E. Ft. Lowell Rd., Suite 106 Tucson, AZ 85719, crown@psi.edu.

Introduction: Two terrestrial craters of different origins have been selected as field sites for this continuing work: El Elegante Crater, a maar crater in the Pinacate Volcanic Field (PVF) in northern Mexico, formed approximately 150,000 years ago from phreatomagmatic explosions [1-2], and Meteor Crater, an impact crater located in central Arizona, formed approximately 50,000 years ago from the impact of an iron nickel meteorite [3]. Both craters are located in arid regions and were selected due to their similarity in size, age, and climate history since formation [4].

The purpose of this work is to determine if formational and sediment transport processes can be established from remote sensing datasets, with field ground-truthing, in a terrestrial setting. Methodologies to distinguish and characterize small crater formational and modification processes, which can be applied to Mars datasets, will then be developed. For this reason, terrestrial remote sensing datasets similar to those currently or soon to be available from Mars were selected for the study of these two craters [3].

Background: Small craters may represent some of the most recent geologic activity on Mars; therefore, quantifying formational and post-formation modification processes associated with these craters may have implications for understanding climate and surface evolution [4, 5]. Because maar craters are created by phreatomagmatic eruptions, the ability to recognize and distinguish them from small impacts remotely is integral in ascertaining the possible role of volatiles in Mars surface processes.

Previous remote sensing work at Meteor Crater has focused on ejecta topography and transport resulting in lithologic unit mapping using linear deconvolution of thermal infrared (TIR) data at varying resolutions [6-8]. Current work expands on this analysis by using datasets over a broader spectral range and higher resolution at Meteor Crater and applies similar methodologies to El Elegante Crater remote sensing datasets. At both sites, the effects of non-mineralogic TIR spectra, small scale features and lithologies, and lithologies of small percentages are considered through the analysis of higher resolution data [4].

Field Data: In June, 2004, and December, 2004, data collection and field observations were conducted at Meteor Crater and El Elegante Crater, respectively. Equipment used included a real-time differential GPS (d-GPS), a laser range finder, a Forward Looking Infrared (FLIR) camera, and a Visible and Near Infrared (VNIR) field spectrometer [4]. Topographic profiles with centimeter horizontal and decimeter vertical accuracy were generated of the crater rims and nearby ejecta fields. Thermal data of ground deposits and crater walls and vegetation spectra were also collected.

Radial transects from the crater rims into near field ejecta were used for topographic data collection and detailed ground cover classification. Sites were established at 50 meter intervals along the transects. Classifications of 2 meter by 2 meter gridded areas were performed in addition to sample collection of surficial fines and small blocks for laboratory spectral analyses and comparison to remote sensing image data. A digital photograph of each site was also taken.

Remote Sensing Data: IKONOS, Hyperion/AVIRIS (AVIRIS for Meteor Crater only), and ASTER data have been collected and analyzed over both Meteor Crater and El Elegante Crater, as well as compared to field-based data.

IKONOS is a 4 band VNIR satellite based imager that produces 1m resolution Geo product datasets. It was chosen for this study due to its similarity to both Mars Orbiter Camera (MOC) with 1.4m resolution and High Resolution Imaging Science Experiment (HiRISE) with sub meter resolution. MOC is currently imaging Mars from the Mars Global Surveyor satellite and HiRISE is part of the Mars Reconnaissance Orbiter instrument package due to arrive in March, 2006.

Hyperion is a hyperspectral Earth Observing-1 (EO-1) satellite instrument that covers a VNIR and short wave infrared (SWIR) spectral range from 0.357 to 2.576μm over 220 bands with a 30m resolution. In addition to Hyperion, Airborne Visible/Infrared Imaging Spectrometer (AVIRIS) data, a hyperspectral airborne instrument covering a range from 0.4 to 2.5 μm over 224 bands with 5m resolution data is available for Meteor Crater. These datasets were selected for their similarity to the Compact Reconnaissance Imaging Spectrometer (CRISM) also aboard the Mars Reconnaissance Orbiter due for Mars arrival in March, 2006. CRISM covers a spectral range of 0.370 to 3.920 μm over 560 bands with 18m resolution.

The Advanced Spaceborne Thermal Emission and Reflection Radiometer (ASTER) is a 14 band multispectral VNIR (3 bands), SWIR (6 bands), TIR (5 bands) instrument aboard the Terra satellite with 15m, 30m, and 90m resolution, respectively. The VNIR and

TIR datasets from ASTER correlate well with the Thermal Emission Imaging System (THEMIS) currently orbiting Mars aboard the Mars Odyssey spacecraft. THEMIS is a multispectral instrument with 5 bands in the VNIR and 9 bands in the TIR spectral range. ASTER also provides a Digital Elevation Model (DEM) dataset using an optical stereo data pair through Band 3 at a 30m resolution and approximately 10m vertical accuracy. The Mars Orbiter Laser Altimeter (MOLA) aboard the Mars Global Surveyor spacecraft has provided a global dataset with 130m resolution and 10m of vertical accuracy.

Results: Integrating field-based observations and data with satellite datasets has provided insight regarding morphology and ejecta characteristics, including the distribution of block sizes with distance from the crater rim, calculation of ejecta volumes from DEMs vs. field-based data, and the effects of juvenile volcanic material on ejecta volume. In addition, we have examined spectral vegetation removal, mineralogic mapping, and thermal interpretation of FLIR data and its relevance to crater wall stratigraphy and ejecta thermal inertia.

From field classifications, block sizes and abundances versus fines abundances have been recorded and compared between craters (Figure 1). At El Elegante Crater, friable deposits of pre-existing altered volcanics were pierced by the vent and easily torn loose during eruptions; ejecta from depths much greater than the exposed stratigraphy is evident in the surrounding deposits [1]. At Meteor Crater, similar to many craters observed by MOC [9], coherent strata is evident in the crater walls despite asymmetric uplift of the rim due to structural control by regional faults [3]. Over 500m of transect distances, El Elegante deposits consistently exhibit larger sizes and quantities of blocky material when compared to Meteor Crater deposits along similar rim transects. Considering fracturing of overlying rock that can take place due to volatile propagated cracks in phreatomagmatic volcanic environments [10], pre-fracturing of the overlying strata may be a factor in generating observed block sizes at El Elegante Crater.

Comparison of field generated topographic profiling to ASTER DEMs demonstrates that there is a difference in calculation of ejecta/crater rim volume (Figure 2). An important consideration is that ejecta volumes using field data has been generated from only 4 transects at each crater, however, resolution is sub meter both vertical and horizontal. ASTER DEMs volumes are calculated from the entire crater rim, but are subject to a 30m resolution constraint.

Both the IKONOS high resolution VNIR dataset and the other lower resolution datasets clearly indicate the gullied eroded tuff south of El Elegante. The asymmetry of the juvenile deposit in relation to the crater is a significant differentiation factor in comparing El Elegante and Meteor Crater. The presence of the largest block sizes on the northeastern rim indicate the vent location was northeast of the crater center, but fines removal has left armored lag deposits there [1]. Meteor Crater does not have a similar asymmetry in its primary ejecta deposit.

Vegetation types and percentage of surface cover were gathered through field observations and site classification. On average, Meteor Crater is 5-10% vegetated and El Elegante Crater is 15-20% vegetated. Using statistical techniques, vegetation masks have been generated to remove vegetative spectra from the datasets creating a lithologically uncontaminated dataset for more accurate mineralogic mapping. Spectral analysis of samples in the University of Pittsburgh's Image Visualization and Infrared Spectroscopy Laboratory has been used for end-member generation and remote spectral comparison to laboratory spectra.

FLIR data at both craters demonstrates differing inertial characteristics between blocks and fines based on particle size, but there is also an indication of differences based on composition in comparing different stratigraphic unit components. Analysis of this dataset continues and may lead to a geographically local thermal inertia model for each crater applicable to Mars data for similar small craters.

References: [1] Gutman, J.T. (1976) *GSA Bull., 87*, 1718-1729. [2] Greeley R. et al. (1985) *NASA Con. Rep. 177356*, 44 pp. [3] Shoemaker E.M. (1960) *Princeton Univ. Press*, 55 pp. [4] Peet, V.M. et al. (2005), *LPS XXXVI,* Abstract 2080. [5] Ramsey, M.S. and D.A. Crown (2004), *LPS XXXV,* Abstract #2031. [6] Ramsey M.S. (2002) *JGR, 107*, doi:10.1029/2001JE001827. [7] Wright S.P. and Ramsey M.S. (2002) *LPI 1129*, 91-92. [8] Wright S.P. and Ramsey M.S. (2003) *LPI XXXIV*, Abstract 1495. [9] Malin M.C. and Edgett K.S. (2000) *Science, 288*, 2330-2335. [10] C.R. Carrigan (2000) *Enc Volc, Academic Press 219-235.*

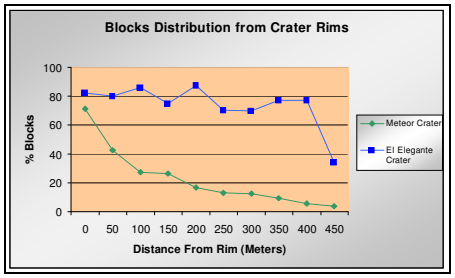

Figure 1. Block distribution from crater rim, Meteor Crater, El Elegante Crater

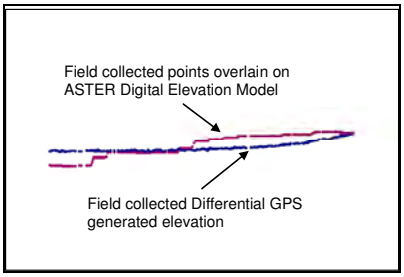

Figure 2. ASTER DEM vs. field topographic profile, Meteor Crater